Control of Magnetic Anisotropy in (Ga, Mn)As by Lithography-Induced Strain Relaxation

J. Wenisch,[1] C. Gould,[1] L. Ebel,[1] J. Storz,[1] K. Pappert,[1] M. J. Schmidt,[1] C. Kumpf,[2] G. Schmidt,[1] K. Brunner,[1] and L. W. Molenkamp[1]

[1]*Physikalisches Institut (EP3), Universität Würzburg, Am Hubland, D-97074 Würzburg, Germany*
[2]*Physikalisches Institut (EP2), Universität Würzburg, Am Hubland, D-97074 Würzburg, Germany*
(Received 22 December 2006; published 14 August 2007)

We report control of magnetic anisotropy in epitaxial (Ga, Mn)As by anisotropic strain relaxation in patterned structures. The strain in the structures is characterized using reciprocal space mapping by x-ray techniques. The magnetic anisotropy before patterning of the layer, which shows biaxial easy axes along [100] and [010], is replaced by a hard axis in the direction of large elastic strain relaxation and a uniaxial easy axis in the direction where pseudomorphic conditions are retained.

DOI: 10.1103/PhysRevLett.99.077201 PACS numbers: 75.50.Pp, 75.30.Gw

The (Ga, Mn)As material system has been the focus of many studies over the past few years. As the understanding of its complex transport and magnetic properties increases, the focus of interest shifts from basic research towards its application in devices. For this, it is necessary to understand how different parameters influence the ferromagnetic material in structures at the device level. In this Letter we present a systematic study of the role of strain relaxation as the dominating factor contributing to the magnetic anisotropy in (Ga, Mn)As nanostructures.

A (Ga, Mn)As layer grown epitaxially on GaAs is subject to compressive strain in the plane of the sample and, at temperatures around 4 K, typically exhibits biaxial in-plane easy axes along [100] and [010] [1,2]. In earlier studies, control of the magnetic anisotropy has been achieved by growing (Ga, Mn)As on a thick, plastically relaxed (In, Ga)As buffer, which induces tensile strain, resulting in an out-of-plane easy axis [3].

Here, we follow an alternative approach in modifying the lattice strain of (Ga, Mn)As on GaAs by lithography, which allows us to *locally* control the magnetic anisotropy of the material. By structuring a fully pseudomorphic 70 nm (Ga, Mn)As layer into thin, elongated stripes, we allow anisotropic, elastic strain relaxation perpendicular to the long axis of the stripe. To increase the strain in the structure compared to the case of (Ga, Mn)As on GaAs, a second sample is processed which includes a highly compressively strained layer acting as an extra stressor to the overlying (Ga, Mn)As layer. The uniaxial strain relaxation in the structures is investigated by grazing incidence (GIXRD) and high-resolution (HRXRD) x-ray diffraction. To determine the influence of patterning on the magnetic anisotropy, a series of magnetometric and magnetotransport studies are performed. We also present finite-element simulations of anisotropic strain relaxation and $\boldsymbol{k} \cdot \boldsymbol{p}$ calculations which confirm the relationship between the structural and magnetic behavior observed in our samples.

The samples are grown in a III-V molecular-beam epitaxy chamber with effusion cells for Ga, In, Mn, and a valved As_4 cell. A 200 nm thick high-quality GaAs buffer is deposited at $T_S = 620\,^\circ$C, on an epiready semi-insulating (001)GaAs substrate, to improve surface and layer quality. During a growth interruption, the temperature is reduced to $270\,^\circ$C. At this temperature, a (Ga, Mn)As layer of 70 nm thickness is deposited at a rate of 0.86 Å/s and a beam equivalent pressure ratio of $As_4/Ga = 25$. The Mn content is determined by HRXRD to be ~2.5% [4]. For one sample, an additional 80 nm thick (In, Ga)As layer with 7.4% In was grown at $500\,^\circ$C prior to (Ga, Mn)As deposition.

After growth, electron beam lithography and chemically assisted ion beam etching are used to pattern both samples into the structure shown in Fig. 1(a). A total area of 4×4 mm is covered by arrays of stripes, each individual stripe measuring nominally 200 nm $\times$ 100 μm with a separating distance of 200 nm. The etch depth is about 200 nm, extending well into the GaAs buffer. The stripes are aligned along the [100] crystal direction.

To optimize the stripe dimensions, the relaxation of the stripes has been modeled by finite-element simulations prior to sample preparation. The simulation makes use of elasticity theory to describe the strain and displacements in the stripe structure by minimizing strain energy. A typical cross section of a relaxed stripe is displayed in Fig. 1(b). Simulations for varied stripe dimensions at fixed material composition suggest that a spatially rather homogeneous

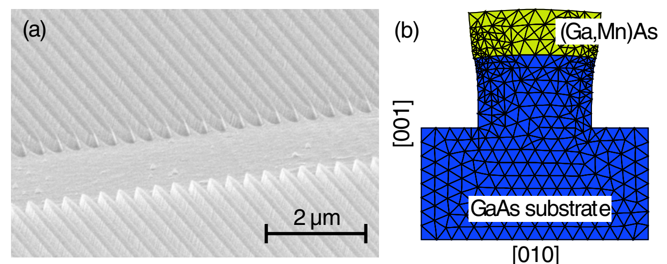

FIG. 1 (color online). (a) Scanning electron microscopy picture of the sample surface after patterning. (b) Simulation of the lattice displacement (100 times exaggerated) after strain relaxation in a cross section of a 200 nm wide stripe.

 © 2007 The American Physical Society

elastic relaxation of the (Ga, Mn)As stripe core is obtained for stripe widths below ~500 nm, while inhomogeneous strain relaxation, concentrated primarily at the edges of the stripe, is observed for wider structures. The etch depth also plays an important role in the degree and homogeneity of strain relaxation. As the substrate pillar height is reduced, the relaxing layer is more restricted at the lower interface resulting in reduced relaxation and a strain gradient along the [001] direction.

The actual strain relaxation in the (Ga, Mn)As stripes is determined from GIXRD reciprocal space mapping in the vicinity of the (333) Bragg reflection. The GIXRD experiments have been performed at beam line BW2 of HASYLAB, using a photon energy of $h\nu = 9.6$ keV and an incidence angle of $\alpha_i = 0.2°$. Because of the small lattice mismatch between GaAs and (Ga, Mn)As of $f = 1.5 \times 10^{-3}$, the Bragg reflections of both materials lie very close to each other. If the (Ga, Mn)As stripes were purely pseudomorphically strained, the difference between both reflections would be only $\Delta l = 0.0044$ r.l.u. (reciprocal lattice units), a value which can hardly be resolved with our experimental setup. However, since the height of the stripes is only about 70 nm, the (Ga, Mn)As (333) reflection is significantly broadened in l direction and fringes due to the finite thickness are visible. Therefore, by mapping the reciprocal space on the maximum of one of the finite thickness fringes, which is far enough from the l position of the GaAs bulk peak, one is mainly sensitive to the (Ga, Mn)As stripes. This measurement, a h-k map at $l = 2.98$, is shown in Fig. 2(a), and a similar map through the GaAs (333) bulk peak in Fig. 2(b). In the stripes-sensitive measurement, one can clearly observe [Fig. 2(a)] a shift of the peak towards smaller values in k. This shift indicates relaxation of the (Ga, Mn)As structure in [010] direction, whereas in [100] direction no relaxation takes place (no peak shift visible in h direction). The different widths of the peaks in h and k direction are due to the different lateral dimensions of the stripes.

In order to quantify the shift, we fit the measured peaks to Voigt profiles. Figure 2(c) shows the central line scan through the peaks of both reciprocal space maps (open circles in the figure). Each curve is fit with the sum of two Voigt peaks (thick solid lines), one fixed at $h = 3$ representing the bulk contribution, the other with a variable position. All four individual peaks are also shown as thin lines. By this procedure we obtain a value for the strain in [010] direction of $\epsilon_{[010]} = (a_s - a_r)/a_r = -2.8 \times 10^{-4}$, where a_s (a_r) is the lattice constant of strained (fully biaxially relaxed) (Ga, Mn)As, respectively. We conclude that the (Ga, Mn)As stripes are pseudomorphically strained in the [100] direction but show a large degree of strain relaxation in the [010] direction.

For magnetic characterization, a superconducting quantum interference device (SQUID) is used to measure the magnetization behavior in the parent and patterned layers. The results are shown in Fig. 3. Note that parent and patterned layers are measured on different pieces of the same wafer, leading to a difference in saturation magnetization between the two experiments.

The parent layer [inset (a) of Fig. 3] exhibits the well-known [1,2] biaxial anisotropy at 4 K, with easy axes loops along the [100] and [010] crystal directions and hard axes

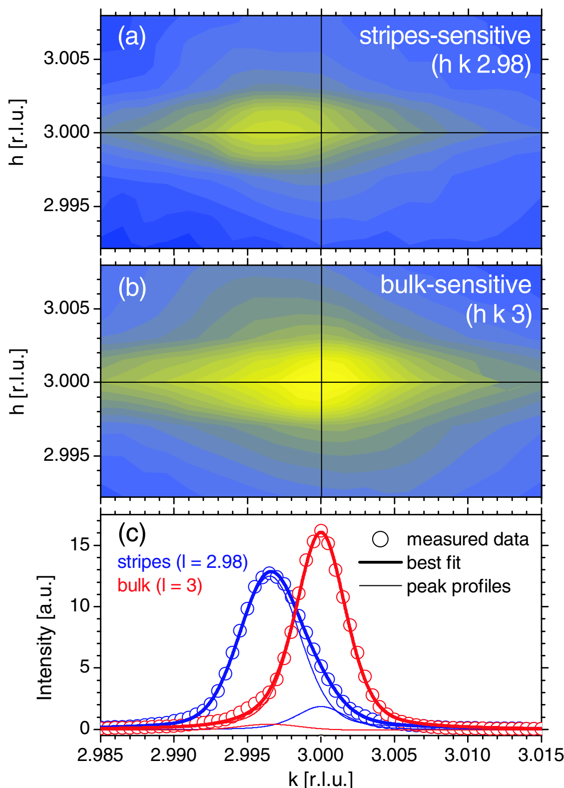

FIG. 2 (color online). Reciprocal space h-k maps in the vicinity of the (333) Bragg reflection at (a) a stripes-sensitive and (b) a bulk-sensitive l position. In (c) the corresponding k-line scans [horizontal scans through the maximum of (a) and (b)] and best fitting Voigt profiles are shown; see text.

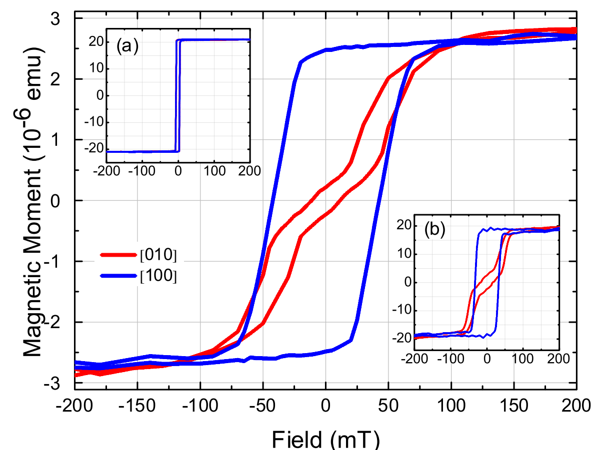

FIG. 3 (color online). SQUID magnetization data at 4 K for the parent layer [inset (a)] and the patterned layer, stripes aligned along [100]. Inset (b) shows the patterned layer data for an additionally strained stripe structure (see text).

along [1$\bar{1}$0] and [110]. The two easy axes are both plotted in the inset (indistinguishable in this graph). Figure 3 shows the anisotropy after patterning. Along the [010] direction, the magnetic moment at zero field drops by ~90% compared to the [100] direction. This previously easy axis is now clearly a very hard magnetization axis. The magnetization reversal along the remaining easy axis [100] takes place circa the uniaxial anisotropy field, as is characteristic of reversal in the single domain limit. As will be confirmed with the transport measurements, magnetization reversal in the patterned structure is governed by coherent Stoner-Wohlfarth rotation, as opposed to domain wall nucleation and propagation in the parent layer. This is reflected by an increase in coercive field from 4 mT in the parent layer to 43 mT in the patterned layer. Thus, the presented results show a clear modification of the magnetic anisotropy of nanopatterned (Ga, Mn)As/GaAs stripes.

The observed strong anisotropy cannot be explained by shape anisotropy. As-grown (Ga, Mn)As shows mainly biaxial crystalline magnetic anisotropy ($K_{\rm cryst} \sim 3000$ J/m^3, as determined for the actual sample by SQUID magnetometry measurements in the hard directions). This dominates the magnetic reversal behavior. Calculating the uniaxial term stemming from the shape anisotropy produced by our geometry (ferromagnetic prism [5]) leads to $K_{\rm shape} \sim 280$ J/m^3, much smaller than the crystalline anisotropy contribution. Thus we attribute the observed emergence of the dominant uniaxial anisotropy in our samples to the anisotropic strain relaxation which, as we show in the $\boldsymbol{k} \cdot \boldsymbol{p}$ modeling below, contributes an additional term in the magnetostatic energy equation, with enough impact to overcome the otherwise dominant biaxial anisotropy.

It is possible to increase the strength of the uniaxial anisotropy by increasing the strain in the parent layer. For this we use a 80 nm (In, Ga)As layer with considerably larger lattice mismatch of $f = 5.3 \times 10^{-3}$ to the substrate, deposited prior to the (Ga, Mn)As layer with $f = 1.5 \times 10^{-3}$. This layer, which is grown to a thickness close to but below the critical value for plastic strain relaxation, acts as a stressor to the overlying (Ga, Mn)As layer.

In Fig. 4 we present HRXRD data of the patterned stripe structure. To distinguish between the lattice constants perpendicular to the long axis of the stripes ([010] direction) and along the stripes ([100] direction), two reciprocal space maps of the (026) and (206) Bragg reflection were taken, with the incident x-ray beam perpendicular [Fig. 4(a)] and parallel [Fig. 4(b)] to the stripes. The relaxation triangle [6,7] of the (In, Ga)As stressor layer indicated in the figure is a convenient method to asses strain relaxation in semiconductor heterostructures and can be applied here because of the relatively large difference in lattice constant between (In, Ga)As stressor layer and GaAs substrate. The difference in position of the (In, Ga)As related peaks in both maps is unambiguous evidence for a large uniaxial strain relaxation in the [010] direction, while retaining fully pseudomorphic conditions along the [100] direction. The peak from the (Ga, Mn)As layer is hardly resolved in these maps, due to its proximity to the bulk GaAs reflection, but is expected to have similar in-plane lattice constants as the (In, Ga)As stressor. From this argument, we conclude that a tensile strain in the range of $\epsilon = (2.2 \pm 1.0) \times 10^{-3}$ has been induced by the (In, Ga)As stressor layer. Magnetically, this sample shows a very similar behavior as the (Ga, Mn)As sample with a GaAs buffer layer, exhibiting biaxial easy axes in the parent layer, and a strong uniaxial anisotropy after patterning [Fig. 3, inset (b)].

The fact that the imposed uniaxial anisotropy in the sample containing the (In, Ga)As layer stressor is consequently stronger than in the first sample can be inferred

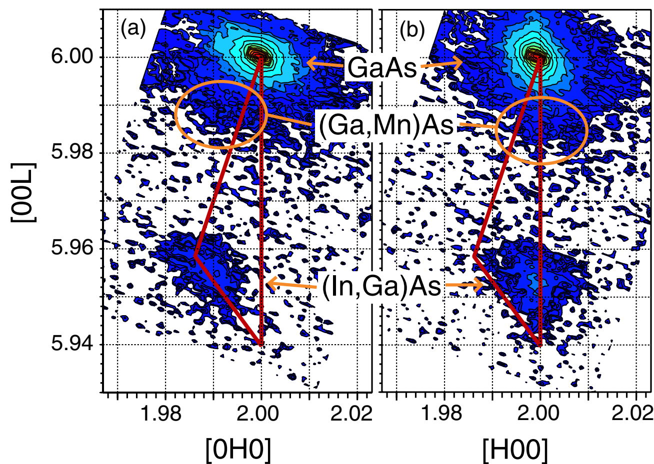

FIG. 4 (color online). Reciprocal space maps of the (026) and (206) Bragg reflection with incident x rays (a) perpendicular and (b) parallel to the stripe axis. The solid dark gray (red) line indicates the triangle of relaxation for uniaxial relaxation.

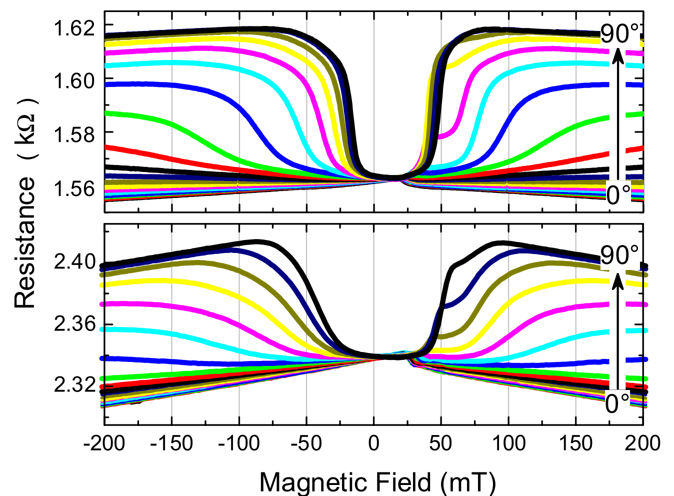

FIG. 5 (color online). Magnetoresistance scans of (Ga, Mn)As/GaAs (top) and (Ga, Mn)As/(In, Ga)As/GaAs stripes (bottom) at 4 K for angles ϕ between magnetic field and current direction (along stripe) from 0° to 90°. The magnetic field is swept from −0.3 to 0.3 T for each scan.

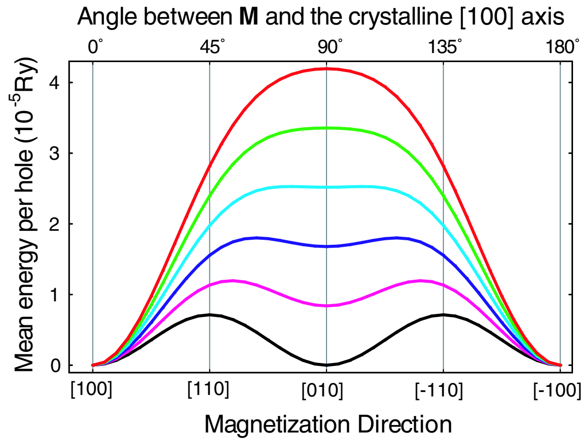

FIG. 6 (color online). Mean energy per valence band hole of a (Ga, Mn)As layer with levels of strain in [010] direction ranging, in equal steps, from the pseudomorphic case ($\epsilon = -1.5 \times 10^{-3}$, bottom, black curve) to the fully relaxed case ($\epsilon = 0$, top, red curve). The strain in [100] remains fixed at $\epsilon = -1.5 \times 10^{-3}$.

from magnetoresistance measurements. In (Ga, Mn)As, which is inherently highly p doped by Mn, a strong anisotropic magnetoresistance is generally observed. The resistance depends on the angle between the magnetization $\vec{M}$ and the current $\vec{J}$ [8], with a minimum when $\vec{M}$ is parallel to the current [9]. For the measurement (see Fig. 5), about 250 parallel stripes are contacted from both ends. A series of magnetic field sweeps from -0.3 to 0.3 T is performed, with incremental increase of the angle ϕ between the magnetic field $\vec{B}$ and $\vec{J}$ after each sweep. In both samples, all (hysteretically symmetric) curves share one low resistance state at $B = 0$ T. When the field sweep is performed in the [100] direction ($\phi = 0°$), the resistance remains at the low state. With increasing angle, a high resistance state develops at high fields and reaches a maximum for $\vec{B} \perp \vec{J}$. At this angle, the magnetization starts out perpendicular to the stripes (high resistance), gradually relaxes through coherent rotation to become parallel to the current direction at zero field (low resistance), and is forced again to the unfavorable direction perpendicular to the stripes at high positive fields. As with the SQUID results, these findings fit perfectly into the picture of a strain-induced uniaxial magnetic anisotropy. We also observe a larger opening of the curves from the additionally (In, Ga)As-strained stripes (lower part of Fig. 5). This is direct evidence of an increased uniaxial anisotropy term, as more energy is necessary to rotate the magnetization into the unfavorable hard [010] direction. The strength of the uniaxial anisotropy is proportional to the half width of these openings [10] of ~45 mT for the pure (Ga, Mn)As stripes and ~80 mT for the additionally strained stripes. As the strain in the magnetic layer of the second sample is demonstrably significantly different, with nominally identical physical dimensions, this effect can clearly be attributed to the lattice strain, considering that shape anisotropy is identical for both structures.

Finally, we present the results of $\boldsymbol{k} \cdot \boldsymbol{p}$ calculations [11] of the magnetization direction dependence of the mean energy per hole. The results support our interpretation that strain is the key element in determining the magnetic anisotropy in (Ga, Mn)As nanostructures. Figure 6 shows the evolution of the equivalent energy minima along [100] and [010] for fully biaxially strained (Ga, Mn)As (black curve) with increasing degree of strain relaxation in the [010] direction. Assuming homogeneous strain in the stripes and a carrier density of 4×10^{20} cm^{-3}, we can deduce from the calculations that the uniaxial contribution from strain dominates over the biaxial term to such a degree that above $\epsilon = -0.6 \times 10^{-3}$ only a single stable point, along [100], remains. This is characteristic of uniaxial behavior. As we demonstrated above in connection with the x-ray data, our patterned samples exhibit strain levels that exceed this number. The difference by a factor of 2 in the anisotropy fields for the two differently strained samples (Fig. 5) also agrees well with the model prediction (we find a factor of 3).

We conclude that our experiments and modeling unambiguously demonstrate that lithographic patterning is a reliable and versatile tool for controlling the magnetic anisotropies in (Ga, Mn)As. We emphasize that this new source of anisotropy arises from the deformation of the crystal structure during relaxation and the strong spin-orbit coupling which links the magnetic properties to the crystal. As such, it is fully distinct from shape or any other form of anisotropy known in metallic ferromagnets. We anticipate that this local technique should prove very useful for device applications.

We thank T. Borzenko, A. Stahl, I. Gierz, and E. Umbach as well as the staff at HASYLAB for their help in this work. We acknowledge financial support from the DFG (BR 1960/2-2 and SFB 410) and the EU (NANOSPIN FP6-IST-015728 and the IHP program "Access to Research Infrastructures").

[1] M. Sawicki *et al.*, Phys. Rev. B **70**, 245325 (2004).
[2] K. Y. Wang *et al.*, Phys. Rev. Lett. **95**, 217204 (2005).
[3] M. Abolfath *et al.*, Phys. Rev. B **63**, 054418 (2001).
[4] G. M. Schott *et al.*, Appl. Phys. Lett. **82**, 4678 (2003).
[5] A. Aharoni, J. Appl. Phys. **83**, 3432 (1998).
[6] H. Heinke *et al.*, J. Phys. D: Appl. Phys. **28**, A104 (1995).
[7] C. Schumacher *et al.*, J. Appl. Phys. **95**, 5494 (2004).
[8] (a) T. R. McGuire and R. I. Potter, IEEE Trans. Magn. **11**, 1018 (1975); (b) J. P. Jan, in *Solid State Physics*, edited by F. Seitz and D. Turnbull (Academic, New York, 1957).
[9] D. V. Baxter *et al.*, Phys. Rev. B **65**, 212407 (2002).
[10] S. Hümpfner *et al.*, Appl. Phys. Lett. **90**, 102102 (2007).
[11] T. Dietl, H. Ohno, and F. Matsukura, Phys. Rev. B **63**, 195205 (2001).